

In situ observation of the phase transformation kinetics of bismuth during shock release

Jiangtao Li(李江涛), Qiannan Wang(王倩男), Liang Xu(徐亮), Lei Liu(柳雷), Hang Zhang(张航), Sota Takagi, Kouhei Ichiyanagi, Ryo Fukaya, Shunsuke Nozawa, and Jianbo Hu(胡建波)

Citation: Chin. Phys. B, 2024, 33 (**4**): 046401. DOI: 10.1088/1674-1056/ad0ec6
Journal homepage: http://cpb.iphy.ac.cn; http://iopscience.iop.org/cpb

What follows is a list of articles you may be interested in

Metal substrates-induced phase transformation of monolayer transition metal dichalcogenides for hydrogen evolution catalysis

Zhe Wang(王喆) and Wenguang Zhu(朱文光)
Chin. Phys. B, 2021, 30 (**11**): 116401. DOI: 10.1088/1674-1056/abfbd1

Novel structures and mechanical properties of Zr_2N: *Ab initio* description under high pressures

Minru Wen(文敏儒), Xing Xie(谢兴), Zhixun Xie(谢植勋), Huafeng Dong(董华锋), Xin Zhang(张欣), Fugen Wu(吴福根), and Chong-Yu Wang(王崇愚)
Chin. Phys. B, 2021, 30 (**1**): 016403. DOI: 10.1088/1674-1056/abb220

Anomalous behavior and phase transformation of α -GaOOH nanocrystals under static compression

Zhao Zhang(张钊), Hang Cui(崔航), Da-Peng Yang(杨大鹏), Jian Zhang(张剑), Shun-Xi Tang(汤顺熙), Si Wu(吴思), Qi-Liang Cui(崔啟良)
Chin. Phys. B, 2017, 26 (**10**): 106402. DOI: 10.1088/1674-1056/26/10/106402

Low-temperature phase transformation of CZTS thin films

Wei Zhao(赵蔚), Lin-Yuan Du(杜霖元), Lin-Lin Liu(刘林林), Ya-Li Sun(孙亚利), Zhi-Wei Liu(柳志伟), Xiao-Yun Teng(滕晓云), Juan Xie(谢娟), Kuang Liu(刘匡), Wei Yu(于威), Guang-Sheng Fu(傅广生), Chao Gao(高超)
Chin. Phys. B, 2017, 26 (**4**): 046402. DOI: 10.1088/1674-1056/26/4/046402

Structure phase transformation and equation of state of cerium metal under pressures up to 51 GPa

Ce Ma(马策), Zuo-Yong Dou(窦作勇), Hong-Yang Zhu(祝洪洋), Guang-Yan Fu(付广艳), Xiao Tan(谈笑), Bin Bai(白彬), Peng-Cheng Zhang(张鹏程), Qi-Liang Cui(崔啟良)
Chin. Phys. B, 2016, 25 (**4**): 046401. DOI: 10.1088/1674-1056/25/4/046401

In situ observation of the phase transformation kinetics of bismuth during shock release

Jiangtao Li(李江涛)[1,2], Qiannan Wang(王倩男)[1,2], Liang Xu(徐亮)[1,2], Lei Liu(柳雷)[1], Hang Zhang(张航)[1,2], Sota Takagi[3,4], Kouhei Ichiyanagi[4], Ryo Fukaya[4], Shunsuke Nozawa[4], and Jianbo Hu(胡建波)[1,2,†]

[1] *Laboratory for Shock Wave and Detonation Physics Research, Institute of Fluid Physics, China Academy of Engineering Physics, Mianyang* 621900, *China*
[2] *State Key Laboratory for Environment-Friendly Energy Materials, Southwest University of Science and Technology, Mianyang* 621010, *China*
[3] *Japan Society for the Promotion of Science, Tokyo*, 102-0083, *Japan*
[4] *Institute of Materials Structure Science, High Energy Accelerator Research Organization (KEK), Ibaraki*, 305-8572, *Japan*

(Received 11 September 2023; revised manuscript received 18 November 2023; accepted manuscript online 22 November 2023)

A time-resolved x-ray diffraction technique is employed to monitor the structural transformation of laser-shocked bismuth. Results reveal a retarded transformation from the shock-induced Bi-V phase to a metastable Bi-IV phase during the shock release, instead of the thermodynamically stable Bi-III phase. The emergence of the metastable Bi-IV phase is understood by the competitive interplay between two transformation pathways towards the Bi-IV and Bi-III, respectively. The former is more rapid than the latter because the Bi-V to B-IV transformation is driven by interaction between the closest atoms while the Bi-V to B-III transformation requires interaction between the second-closest atoms. The nucleation time for the Bi-V to Bi-IV transformation is determined to be 5.1±0.9 ns according to a classical nucleation model. This observation demonstrates the importance of the formation of the transient metastable phases, which can change the phase transformation pathway in a dynamic process.

Keywords: phase transformation, time-resolved x-ray diffraction (XRD), bismuth, metastable phase, nonequilibrium phase diagram

PACS: 64.70.K–, 64.60.My, 62.50.Ef **DOI:** 10.1088/1674-1056/ad0ec6

1. Introduction

Structural transformations in a dynamic process are of great concern because the associated properties (such as mechanical,[1,2] optical,[3–5] electrical[6,7] ones) may change abruptly and evolve in a different pattern from then on. These transformations are usually non-equilibrium in nature,[8] proceeding in nanosecond or even picosecond timescales[9–15] with the kinetics different from the one in the equilibrium case.[16] Fully understanding the transformation kinetics, especially its rate dependence, under dynamic compression has been a long-term pursuit in the field of materials dynamics.

Bismuth, a prototype for the study of phase transitions under high pressure, has been intensively investigated by both static and dynamic compression techniques.[17–23] Even though bismuth has a complex phase diagram including multiple polymorphisms, its equations of state,[21–23] crystal structures[22–24] and phase boundaries[25–27] at equilibrium have been well clarified with both experimental and theoretical efforts. When the loading or unloading rate is non-negligible compared to the rate of phase transformations, the kinetic effect needs to be considered. The kinetics of phase transformations and the transformation pathways are by far much less understood.[16,17,28–31] Generally speaking, the transformation pathway in the dynamic process could be different from one predicted using the equilibrium phase diagram by shifting the phase boundaries towards the loading direction.[30] However, the formation of transient metastable phases in the dynamic process[16,28,29] significantly changes the landscape of dynamic phase transformation, making it unreliable to interpret the data from traditional shock wave experiments based only on the equilibrium phase diagram. For bismuth, it is found that the phase transformation follows a pathway across the static phase diagram with phase boundaries shifted by the kinetics when the loading and unloading processes are performed in a timescale of milliseconds,[20,30] but adopts another pathway with metastable phases deeply engaged in a timescale of nanoseconds.[16,28,29] The differences between the phase transformation pathways in the two timescales highlight the importance of investigating the phase transformation kinetics of bismuth, especially the kinetics associated with metastable phases.

In order to gain a better understanding of the transformation kinetics of bismuth, in this study, we employ a time-resolved x-ray diffraction (XRD) technique to monitor the structural change of bismuth in the shock release period with the controlled decreasing rate of pressure. A retarded transformation from the shock-induced Bi-V phase to a metastable phase has been observed in the release period with the phase identified as metastable Bi-IV. The mechanism for the formation of the metastable Bi-IV instead of the thermodynamically

†Corresponding author. E-mail: jianbo.hu@caep.cn

© 2024 Chinese Physical Society and IOP Publishing Ltd

stable Bi-III phase is discussed from the perspective of phase transformation kinetics.

2. Experiment

Experiments were performed at the beamline NW14A of the Photon Factory Advanced Ring (PF-AR) of the High Energy Accelerator Research Organization (KEK). The schematic of the experimental setup is shown in Fig. 1(a). Experimental details are given in Ref. [32]. Briefly, the target assembly consists of four layers, a 25 μm thick polyethylene terephthalate (PET) layer, a glue layer with a mean thickness of 20 (±2) μm, and an 8 μm thick bismuth film deposited on a 100 μm thick LiF single crystal window. A flat-top ablation laser with a temporal Gaussian pulse duration of 12 ns and a pulse energy of 10.7 (±0.1) J is focused on the PET layer with the spot diameter of 450 μm to generate loading waves, which propagate forward to compress the sample. A 15.6 keV ($dE/E = 1.3\%$) x-ray pulse outputted from the synchrotron is used to probe the compressed state of the sample, generating an XRD pattern on the CCD detector (MarCCD 165, Rayonix, LLC). The pulse width of the x-ray beam, constraining the temporal resolution of the XRD technique, is 100 ps. The x-ray beam size at the sample position is tailored by slits to be 460 μm (H)×240 μm (V), with about 98% of the x-ray photons passing through the loaded sample. Considering the sample-to-detector distance of 93.912 mm, the angular resolution is expected to be around 0.3°. By manipulating the delay time between the laser shock and the x-ray probe, time-resolved XRD spectra of bismuth in the compression and release period are obtained.

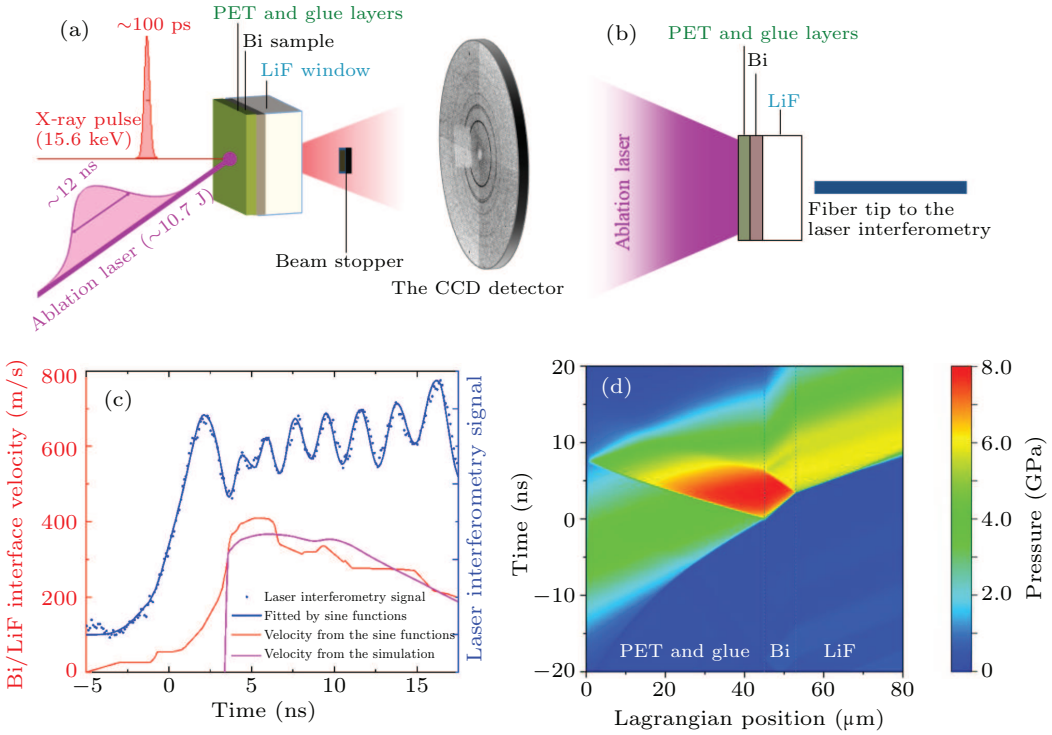


Fig. 1. (a) Schematic of the experimental setup for time-resolved XRD measurement. (b) Schematic of the experimental setup for the Bi/LiF interface velocity measurement. (c) The Bi/LiF interface velocities obtained from the periodical laser interferometry signal and from the hydrodynamic simulation. (d) A 1D hydrodynamic simulation of the laser loading and unloading process.

In order to quantify the stress history that the Bi sample underwent, a laser interferometry system[33,34] is employed to monitor the interfacial particle velocity profile between the Bi sample and the LiF window, as shown in Fig. 1(b). The interferometry data are fitted by a series of sinusoidal functions. The interfacial velocity is then obtained from the derivative of the phase in the sinusoidal function with respect to time,[35] taking into account the correction due to the refractive index of the LiF window.[36,37] As shown in Fig. 1(c), the peak velocity is 0.41±0.02 km/s, corresponding to the peak stress of 7.9±0.4 GPa. Thereafter, the interfacial velocity decreases gradually over about 10 ns, indicating a low decreasing rate of the pressure in Bi. This is also confirmed by the 1D hydrodynamic simulation using MULTI-1D,[38] as shown in Fig. 1(d). To simplify the simulation, a single-phase Grüneisen equation of state for Bi ($\rho_0 = 9.84$ g/cm^3, $c_0 = 1.83$ km/s, $\lambda = 1.47$, $\gamma_G = 1.1$) is employed. The ramping slope in the increase of the velocity profile, which failed to be captured by the simulation, is possibly due to elastic precursors and phase transformations. Afterwards, the velocity profile shows a long release period, which is in fairly good agreement with the simulation despite the simplicity of the equation of state model. According to the simulation, the long release period is associated with the long pulse duration of the ablation laser. As the laser intensity enters the decreasing phase of the Gaussian profile, the release waves produced at the ablation side start to attenuate

the pressure inside the sample. The decreasing rate of the pressure in the sample was held to keep pace with the decreasing rate of the laser intensity, resulting in a much longer release period than those reported previously.[28,29,31]

3. Results and discussion

After integrating the intensity of the diffraction patterns recorded on the CCD at each probing time (see Fig. S1 in the supplementary material for the raw CCD images), time-resolved XRD spectra of bismuth under laser-driven shock compression are shown in Fig. 2(a). The x axis is the momentum transfer $Q = 4\pi \sin\theta/\lambda$, where θ is the Bragg angle. The static diffraction spectrum shows that the Bi-I phase is the primary phase before the laser compression. We set the time to zero when the shock wave enters the bismuth film. At $t = 1.2$ ns, a new peak at $Q = 2.3$ Å^{-1} appears corresponding to the Bi-V phase, and the peak at $Q = 1.9$ Å^{-1} shows contributions from both the uncompressed and compressed Bi-I phase, indicating that part of the sample is compressed and transforms into the Bi-V phase following the propagation of the compression wave. The pressure of the Bi-V phase is determined to be 7.9 GPa from the measured velocity profile. At $t = 4.3$ ns, the peak at $Q = 1.9$ Å^{-1} nearly disappears and the peak at $Q = 2.3$ Å^{-1} becomes the dominant one, indicating that the compression wave turns nearly the whole sample into the Bi-V phase. Moreover, two other characteristic peaks of the Bi-V phase at $Q = 3.2$ Å^{-1} and 3.9 Å^{-1} become notable. In the delay times at $t = 6.9$ ns, 10.7 ns, 13.7 ns and 17.0 ns, the pressure decreases continuously as indicated by the shift of the peak locations of the Bi-V phase. Meanwhile, another peak with a larger FWHM located at $Q = 2.2$ Å^{-1} keeps increasing the intensity and overtakes the original Bi-V phase peak located at $Q = 2.3$ Å^{-1}. At the same time, weak peaks located at $Q = 2.7$ Å^{-1} and 3.0 Å^{-1} grow synchronously, suggesting the possible nucleation and growth of the Bi-IV phase as identified in Fig. 2(a). At $t = 17.0$ ns, the characteristic peaks of the Bi-V phase disappear and the peak located at $Q = 2.2$ Å^{-1} becomes dominant, indicating that the transformation from Bi-V to the metastable phase is nearly finished.

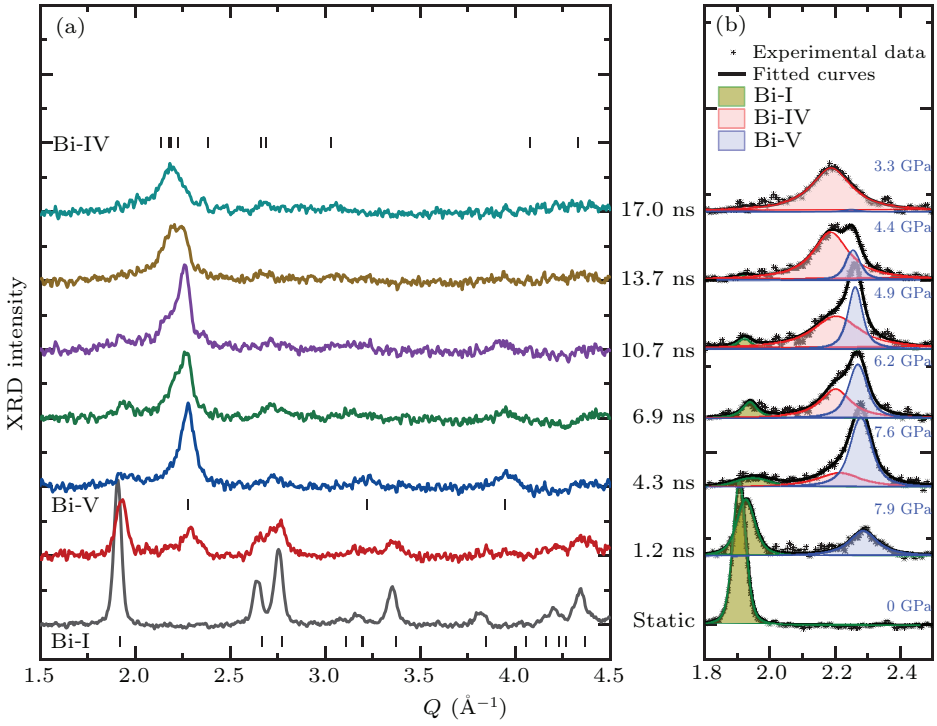


Fig. 2. (a) Time-resolved XRD spectra of bismuth under laser-driven shock compression with the notable diffraction spots of the LiF single crystal removed before performing the integration. (b) A zoomed-in view of XRD peak profiles in the Q range of 1.8–2.5 Å^{-1} with the fitting curve by Voigt functions, showing the phase transformation from the Bi-V to the Bi-IV phase in the release period.

To strengthen this identification, a comparison of the XRD spectrum at $t = 17.0$ ns where the metastable phase becomes dominant with the spectra of possible candidates, such as the Bi-IV,[25] Bi-III,[20] Bi-II′[28] and Bi-II[23] phases from the literature, are shown in Fig. 3. Apart from a minor contribution of the Bi-II phase, with XRD peaks located at $Q = 2.0$ Å^{-1} and $Q = 2.3$ Å^{-1}, formed probably due to the irremovable pressure gradient as suggested by Gorman *et al.*,[29] the other XRD peak features, including the dominant peak located at $Q = 2.2$ Å^{-1} and other minor peaks located at $Q = 2.7$ Å^{-1} and 3.0 Å^{-1}, can be well approximated using the peak features of the Bi-IV phase. There are probably two reasons for the broadening of the diffraction peak located at $Q = 2.2$ Å^{-1}. One is that the new phase was still in its infancy, with the grain sizes so small that the crystal structure was easily deformable due to external stress. Another reason

is that the pressure gradient, which was increasing with time, generated a broadened diffraction peak. This observation is consistent with the result obtained by Gorman *et al.* using high-flux XFEL beams (see Fig. S4 in Ref. [16]), although they suggest that the metastable phase is different from the Bi-IV phase due to the absence of a weak diffraction peak located at $Q = 2.4$ Å^{-1}.[16] One needs to realize that it is nearly impossible to find a different crystal structure with the same diffraction spectrum but with only one peak missing. Therefore, it is very likely that the missing weak diffraction peak is due to the texture in the transformed Bi-IV phase.

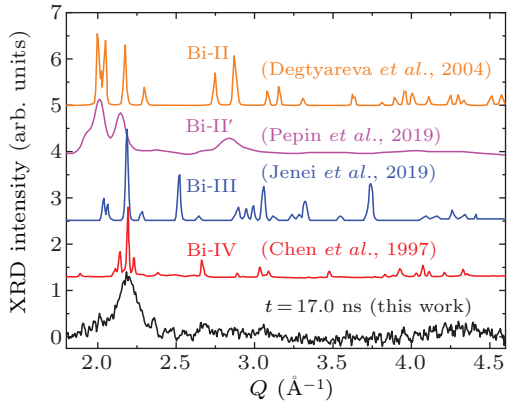


Fig. 3. Comparison of the XRD spectrum at $t = 17.0$ ns obtained in this work with the spectra of the Bi-IV,[25] Bi-III,[20] Bi-II′[28] and Bi-II[23] phases from the literature.

The identification of the target phase as the Bi-IV phase is intriguing if one looks at the equilibrium phase diagram of bismuth.[28] Referring to the phase diagram, it was expected that the Bi-III phase would come into being instead of the Bi-IV phase, as observed in the unloading process performed in the timescale of milliseconds.[30] However, Principi *et al.* reported that the transformation from the Bi-V to the Bi-IV phase may occur when the thermodynamic state enters the stability field of the Bi-III phase along the path of decreasing temperature,[18] as shown in Fig. 4. The formation of the metastable Bi-IV instead of the stable Bi-III phase points to two possibilities for the phase transformation pathways. (1) The structural transformation from the Bi-V to the Bi-III phase 'bypasses' the Bi-IV phase, as in the case of the formation of metastable body-centered cubic (bcc) structure in the pathway of the transformation from close-packed hexagonal (hcp) structure to simple hexagonal (ω) structure upon shock compression of zirconium.[39,40] (2) The structural transformations from the Bi-V to the Bi-IV phase or from the Bi-V to the Bi-III phase are independent, or more precisely competitive, with the former more rapid than the latter, thus resulting in a transient dominance of the metastable Bi-IV phase. To determine the underlying transformation pathway, the displacive mechanisms associated with the two transformations are analyzed in the following diagrams.

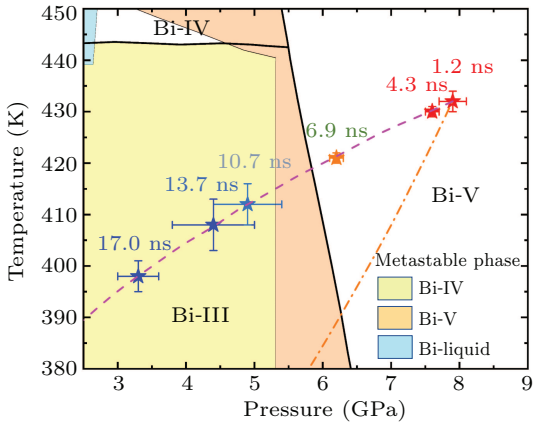


Fig. 4. The thermodynamic and metastable phase diagram of bismuth[18,28] with the Hugoniot and the isentropic release paths denoted by dash-dot and dash lines, respectively. The thermodynamic states probed by the time-resolved XRD technique are represented by scattered stars with filled colors. The gradual change of the colors from red to blue indicates the phase transformations from the Bi-V to the Bi-IV phase in the release period. Both the pressure and the temperature error bars are from the hydrodynamic simulation.

The displacing mechanism associated with the Bi-V to Bi-IV transformation is shown in Fig. 5(a). The Bi-V phase has a bcc structure and the Bi-IV phase is described as a distorted bcc structure.[25,41] The symbols Ai (red), Bi (blue) and Ci (magenta) ($i = 0$, 1, 2, etc.) label the atoms on the first, second and third layers from the perspective shown in Fig. 5(a). It is found that the first layer resembles the third layer after a displacement. The transformation from the Bi-V to the Bi-IV phase can be interpreted as a distortion involving three collective displacements in a unit cell as follows: 1) the movement of B0 atom in the [001] direction; 2) the movement of C1 and C3 atoms towards each other, and that of C2 and C4 atoms against each other; 3) the expansion and rotation of the square formed by Ai ($i = 1$, 2, 3, 4) atoms.

The displacing mechanism associated with the Bi-V to Bi-III transformation[42] is shown in Fig. 5(b). The Bi-III phase has a host-guest (hg) structure with the Ai and Bi ($i = 1$, 2, 3, 4) atoms forming a 'cage' and the B0 atom in the 'cage' center (the slight modulations of the atomic positions are not discussed here for the sake of simplicity). The transformation from the Bi-V to Bi-III phase can also be interpreted from the perspective of 'cage' formation involving three collective displacements as follows: 1) the movement of B0 atom in the [001] direction; 2) the contraction and rotation of the square formed by Bi ($i = 1$, 2, 3, 4) atoms; 3) the expansion and rotation of the square formed by Ai ($i = 1$, 2, 3, 4) atoms.

It is noted that the main difference between the transformation from the Bi-V to Bi-IV or to Bi-III lies on the second collective displacement. Since the atoms are repelling each other under high pressure, for the Bi-V to Bi-IV transformation, the movement of C1 and C3 atoms towards each other is correlated to the movement of B0 atom in the [001] direction to achieve a minimized energy of the crystal. For the Bi-V to Bi-III transformation, the contraction of the square formed by

Bi (i = 1, 2, 3, 4) atoms is correlated to the movement of B0 atom in the [001] direction to achieve a minimized energy of the crystal. The former displacement is driven by the interaction between the closest atoms (C1 and B0, as well as C3 and B0), while the latter is driven by the interaction between the second-closest atoms (Bi and B0, i = 1, 2, 3, 4). We thus suggest that the former displacement is more efficient than the latter, since it causes a faster nucleation of the Bi-IV phase.

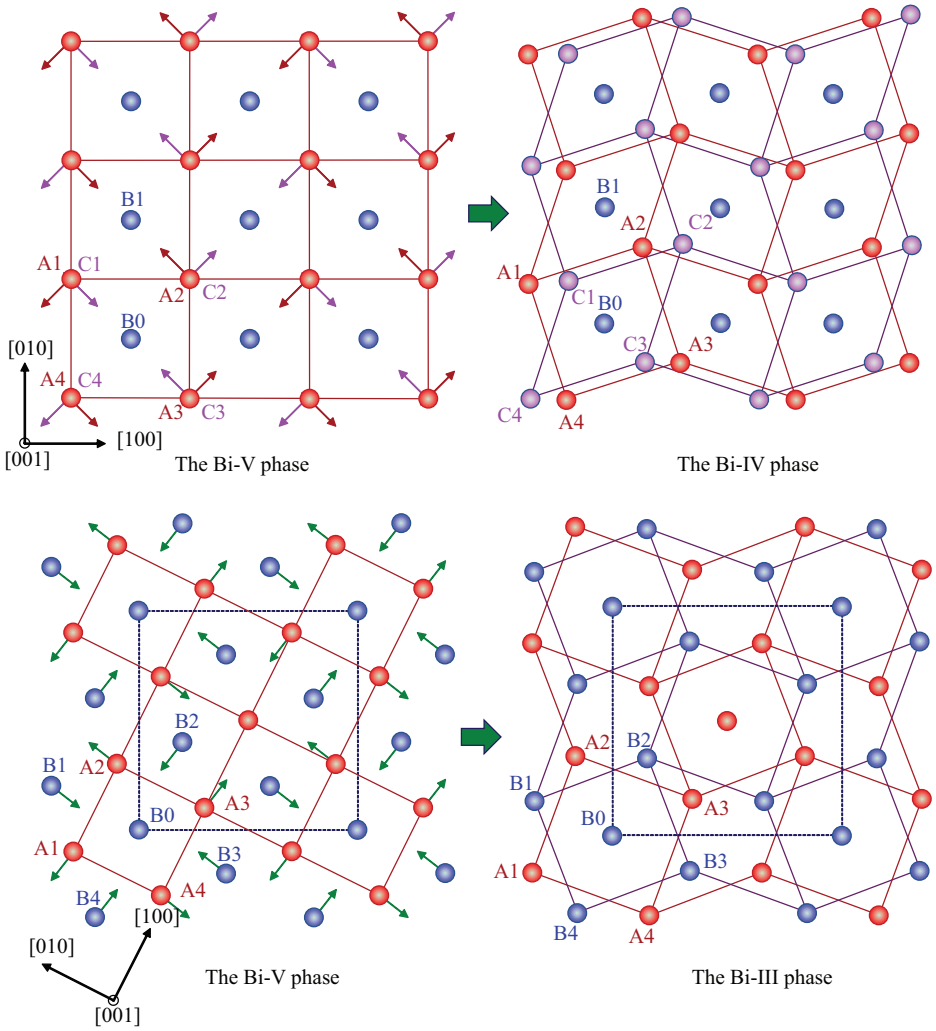


Fig. 5. The displacive mechanisms associated with the Bi-V to Bi-IV transformation (a) and the Bi-V to Bi-III transformation (b).

The faster nucleation of the Bi-IV instead of the Bi-III phase provides an example to illustrate that the nucleation time is more directly related to the gradient of the Gibbs free energy with respect to the collective displacements of the atoms ($\nabla_R G$, R is the coordinates of atoms) rather than the difference in the Gibbs free energy between the parent and child phases (ΔG), which is usually considered as the main driving force for the phase transformation.[8,17] If ΔG was the main driving force for the phase transformation, $\Delta G_{\mathrm{V-III}}$ (the difference in Gibbs energy between the Bi-V and Bi-III phase) is larger than $\Delta G_{\mathrm{V-IV}}$ in absolute value. Thus, the Bi-V to Bi-III transformation should be faster than the Bi-V to Bi-IV transformation. This is not supported by our observations in this study. Whereas, if $\nabla_R G$ is considered to be the driving force for the phase transformation, $\nabla_R G_{\mathrm{V-IV}}$ is larger than $\nabla_R G_{\mathrm{V-III}}$ in absolute value. Thus, the Bi-V to Bi-IV transformation should be faster than the Bi-V to Bi-III transformation, which is in agreement with our observations.

The nucleation time from the Bi-V to Bi-IV phase can be obtained from the increase in the integrated diffraction intensity at $Q = 2.2$ Å^{-1} with time according to a classical nucleation model,[43,44] as shown in Fig. 6(a). Here, the time zero is redefined as when the rarefaction waves from the Bi/LiF interface start to decrease the pressure in the bismuth sample according to the hydrodynamic simulation. The uncertainty in time or more precisely time zero is due to the variation of the glue thickness. According to the Johnson–Mehl–Avrami equation[45–47] in classical nucleation theory, the volume fraction of the Bi-IV phase (ϕ_{IV}) is related to the nucleation time (τ) by $\phi_{\mathrm{IV}} = 1 - \exp(-(t/\tau)^n)$, where n is the growth dimension of the new phase. Assuming a heterogeneous (homogeneous) nucleation, $n = 1$ (2) represents a planar

growth, $n = 2$ (3) represents a cylindrical growth and $n = 3$ (4) represents a spherical growth. In order to determine n as well as τ, the Johnson–Mehl–Avrami equation is rewritten as $\ln(-\ln(1-\phi_{\rm IV})) = n(\ln(t) - \ln(\tau))$[48] with the values of $\ln(-\ln(1-\phi_{\rm IV}))$ and $\ln(t)$ plotted in Fig. 6(b). The linear fit reveals that $n = 2.0$ and $\tau = 5.1$ ns. From the value of n, it is not sufficient to tell whether it is a homogeneous nucleation with a planar growth or a heterogeneous nucleation with a cylindrical growth. The variation of the nucleation time from 4.6 ns to 6.0 ns is shown as the shaded magenta region, giving uncertainty of the nucleation time to be about 0.9 ns. The large nucleation time of the Bi-IV phase in the Bi-V phase provides a constraint on the experimental observation of a dominated Bi-IV phase, suitable for structural identification or construction using the XRD technique. That is, the decreasing rate of pressure should be low enough so that the nucleation of other phases (such as Bi-II, Bi-II′ or Bi-I) does not severely interfere with the nucleation of the Bi-IV phase.

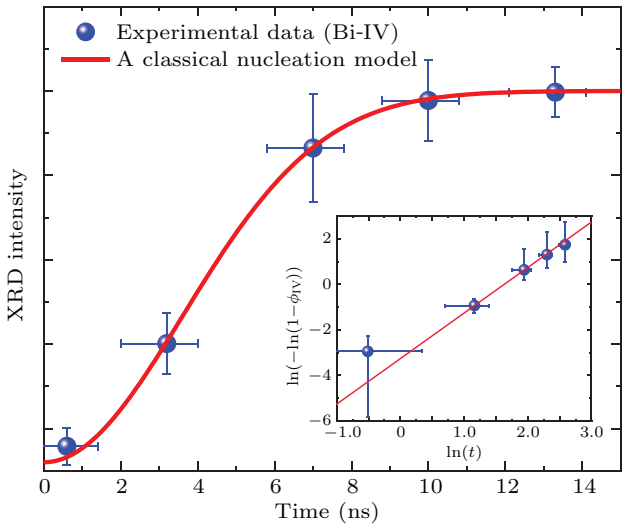


Fig. 6. (a) The increase in the integrated diffraction intensity at $Q = 2.2$ Å^{-1} with time. The result from a classical nucleation model is also shown with the model parameters determined from (b). (b) A comparison of the experimental data with the results from the classical nucleation model. The nucleation time constant is determined to be 5.1 ns (the red line), and its uncertainty is estimated by varying its value from 4.6 ns to 6.0 ns, as shown by the shaded magenta region.

4. Conclusion

The phase transformations of bismuth in a controlled shock release process are monitored by the time-resolved x-ray diffraction technique. The long release period allows the phase transformation kinetics from the Bi-V to a metastable Bi-IV phase to be revealed. The nucleation time for the transformation is determined to be 5.1±0.9 ns, with the growth dimension $n = 2$, suggesting a planar growth in the homogeneous nucleation mode or a cylindrical growth in the heterogeneous nucleation mode. The formation of the metastable Bi-IV instead of the stable Bi-III phase is attributed to the competition between two transformation pathways, in which the Bi-V to Bi-IV transformation is more rapid than the Bi-V to Bi-III transformation, resulting in a transient dominance of the metastable Bi-IV phase. This is supported by an analysis of the collective displacements that the Bi-V to B-IV transformation is driven by the interaction between the closest atoms while the Bi-V to B-III transformation requires the interaction between the second closest atoms. The faster nucleation of the Bi-IV instead of the Bi-III phase points to the fact that the nucleation time is more directly related to $\nabla_R G$ rather than ΔG, which can be helpful for establishing a theoretical model of phase transformation.

Acknowledgements

We thank Prof. Kazutaka G. Nakamura, Dr Shourui Li, Dr Yinghua Li, Dr Junjie Gao and Prof. Lin Zhang for helpful discussions. This study was supported by the National Natural Science Foundation of China (Grant No. 12072331), the Science Challenge Project (Grant No. TZ2018001), the Japan Society for the Promotion of Science (Grant Nos. 17H04820 and 21H01677) and the Foundation of the United Laboratory of High-Pressure Physics and Earthquake Science, and was performed under the approval of the Photon Factory Program Advisory Committee (Proposal Nos. 2016S2-006 and 2020G680).

References

[1] Kraus D, Ravasio A, Gauthier M, *et al*. 2016 *Nat. Commun.* **7** 10970
[2] Turneaure S J, Sharma S M, Volz T J, Winey J M and Gupta Y M 2017 *Sci. Adv.* **3** eaao3561
[3] Knudson M D, Desjarlais M P, Becker A, Lemke R W, Cochrane K R, Savage M E, Bliss D E, Mattsson T R and Redmer R 2015 *Science* **348** 1455
[4] Celliers P M, Millot M, Brygoo S, McWilliams R S, Fratanduono D E, Rygg J R, Goncharov A F, Loubeyre P, Eggert J H, Peterson J L, Meezan N B, Le Pape S, Collins G W, Jeanloz R and Hemley R J 2018 *Science* **361** 677
[5] Hartley N J, Zhang C, Duan X, Huang L G, Jiang S, Li Y, Yang L, Pelka A, Wang Z, Yang J and Kraus D 2020 *Matter Radiat. Extrem.* **5** 028401
[6] McWilliams R S, Spaulding D K, Eggert J H, Celliers P M, Hicks D G, Smith R F, Collins G W and Jeanloz R 2012 *Science* **338** 1330
[7] Eremets M I, Shimizu K, Kobayashi T C and Amaya K 1998 *Science* **281** 1333
[8] Boettger J C and Wallace D C 1997 *Phys. Rev. B* **55** 2840
[9] Hwang H, Galtier E, Cynn H, *et al.* 2020 *Sci. Adv.* **6** eaaz5132
[10] Turneaure S J, Sharma S M and Gupta Y M 2018 *Phys. Rev. Lett.* **121** 135701
[11] Swinburne T D, Glavicic M G, Rahman K M, Jones N G, Coakley J, Eakins D E, White T G, Tong V, Milathianaki D, Williams G J, Rugg D, Sutton A P and Dye D 2016 *Phys. Rev. B* **93** 144119
[12] Bastea M, Bastea S and Becker R 2009 *Appl. Phys. Lett.* **95** 241911
[13] Jensen B J, Gray III G T and Hixson R S 2009 *J. Appl. Phys.* **105** 103502
[14] Barker L M and Hollenbach R E 1974 *J. Appl. Phys.* **45** 4872
[15] Kalita P, Specht P, Root S, Sinclair N, Schuman A, White M, Cornelius A L, Smith J and Sinogeikin S 2017 *Phys. Rev. Lett.* **119** 255701
[16] Gorman M G, Coleman A L, Briggs R, McWilliams R S, McGonegle D, Bolme C A, Gleason A E, Galtier E, Lee H J, Granados E, Śliwa M, Sanloup C, Rothman S, Fratanduono D E, Smith R F, Collins G W, Eggert J H, Wark J S and McMahon M I 2018 *Sci. Rep.* **8** 16927
[17] Smith R F, Eggert J H, Saculla M D, Jankowski A F, Bastea M, Hicks D G and Collins G W 2008 *Phys. Rev. Lett.* **101** 065701

[18] Principi E, Minicucci M, Di Cicco A, Trapananti A, De Panfilis S and Poloni R 2006 *Phys. Rev. B* **74** 064101
[19] Bastea M, Bastea S, Emig J A, Springer P T and Reisman D B 2005 *Phys. Rev. B* **71** 180101
[20] Jenei Z, Liermann H P, Husband R, Méndez A S J, Pennicard D, Marquardt H, O'Bannon E F, Pakhomova A, Konopkova Z, Glazyrin K, Wendt M, Wenz S, McBride E E, Morgenroth W, Winkler B, Rothkirch A, Hanfland M and Evans W J 2019 *Rev. Sci. Instrum.* **90** 065114
[21] Akahama Y, Kawamura H and Singh A K 2002 *J. Appl. Phys.* **92** 5892
[22] McMahon M I, Degtyareva O and Nelmes R J 2000 *Phys. Rev. Lett.* **85** 4896
[23] Degtyareva O, McMahon M I and Nelmes R J 2004 *High Press. Res.* **24** 319
[24] Häussermann U, Söderberg K and Norrestam R 2002 *J. Am. Chem. Soc.* **124** 15359
[25] Chen J H, Iwasaki H and Kikegawa T 1997 *J. Phys. Chem. Solids* **58** 247
[26] Cannon J F 1974 *J. Phys. Chem. Ref. Data* **3** 781
[27] Klement W, Jayaraman A and Kennedy G C 1963 *Phys. Rev.* **131** 632
[28] Pépin C M, Sollier A, Marizy A, Occelli F, Sander M, Torchio R and Loubeyre P 2019 *Phys. Rev. B* **100** 060101
[29] Gorman M G, Coleman A L, Briggs R, McWilliams R S, Hermann A, McGonegle D, Bolme C A, Gleason A E, Galtier E, Lee H J, Granados E, McBride E E, Rothman S, Fratanduono D E, Smith R F, Collins G W, Eggert J H, Wark J S and McMahon M I 2019 *Appl. Phys. Lett.* **114** 120601
[30] Husband R J, O'Bannon E F, Liermann H P, Lipp M J, Méndez A S J, Konôpková Z, McBride E E, Evans W J and Jenei Z 2021 *Sci. Rep.* **11** 14859
[31] Hu J, Ichiyanagi K, Doki T, Goto A, Eda T, Norimatsu K, Harada S, Horiuchi D, Kabasawa Y, Hayashi S, Uozumi S, Kawai N, Nozawa S, Sato T, Adachi S and Nakamura K G 2013 *Appl. Phys. Lett.* **103** 161904
[32] Takagi S, Ichiyanagi K, Kyono A, Nozawa S, Kawai N, Fukaya R, Funamori N and Adachi S 2020 *J. Synchrotron Rad.* **27** 371
[33] Weng J, Wang X, Ma Y, Tan H, Cai L, Li J and Liu C 2008 *Rev. Sci. Instru.* **79** 113101
[34] Nissim N, Greenberg E, Werdiger M, Horowitz Y, Bakshi L, Ferber Y, Glam B, Fedotov-Gefen A, Perelmutter L and Eliezer S 2021 *Matter Radiat. Extrem.* **6** 046902
[35] Chen X H, Zeng X L, Fan D, Liu Q C, Bie B X, Zhou X M and Luo S N 2014 *Rev. Sci. Instrum.* **85** 026106
[36] Fratanduono D E, Boehly T R, Barrios M A, Meyerhofer D D, Eggert J H, Smith R F, Hicks D G, Celliers P M, Braun D G and Collins G W 2011 *J. Appl. Phys.* **109** 123521
[37] LaLone B M, Fat'yanov O V, Asay J R and Gupta Y M 2008 *J. Appl. Phys.* **103** 093505
[38] Ramis R, Schmalz R and Meyer-Ter-Vehn J 1988 *Comput. Phys. Comm.* **49** 475
[39] Gao L, Ding X, Lookman T, Sun J and Salje E K H 2016 *Appl. Phys. Lett.* **109** 031912
[40] Armstrong M R, Radousky H B, Austin R A, *et al*. 2021 *JOM* **73** 2185
[41] Degtyareva V F 2000 *Phys. Rev. B* **62** 9
[42] Katzke H and Tolédano P 2008 *Phys. Rev. B* **77** 024109
[43] Singh A K 1985 *Mater. Sci. Forum* **3** 291
[44] Chandra Shekar N V and Rajan K G 2001 *Bull. Mater. Sci.* **24** 1
[45] Avrami M 1939 *J. Chem. Phys.* **7** 1103
[46] Avrami M 1940 *J. Chem. Phys.* **8** 212
[47] Avrami M 1941 *J. Chem. Phys.* **9** 177
[48] Krüger T, Merkau B, Grosshans W A and Holzapfel W B 1990 *High Press. Res.* **2** 193